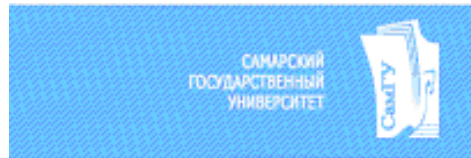


Heavy quarkonium production in the Regge limit of QCD: predictions for Tevatron and LHC colliders

V.A. Saleev and D. V. Vasin

Samara State University, Samara, Russia



in collaboration with

B. A. Kniehl (Hamburg University, Hamburg, Germany)

1. QMRK approach
2. NRQCD
3. Heavy quarkonium production by reggeized gluons
4. Heavy quarkonium production at the Tevatron
5. Heavy quarkonium production at the LHC
6. Conclusion

The QMRK approach

$$\mu \approx M_T = \sqrt{M^2 + |\mathbf{p}_T|^2}$$

In the conventional Parton Model: Dokshitzer-Gribov-Lipatov-Altarelli-Parisi (DGLAP) evolution equation, $\ln(\mu/\Lambda_{QCD})$.

$$S > \mu^2 \gg \Lambda_{QCD}^2, \text{ and } q_T = 0.$$

In the high-energy Regge limit the summation of the large logarithms $\ln(\sqrt{S}/\mu)$ in the evolution equation can then be more important: Balitsky-Fadin-Kuraev-Lipatov (BFKL) evolution equation and $k_T \neq 0$ for *reggeized* t -channel gluons.

$$x = \mu/\sqrt{S} \ll 1$$

As the theoretical framework of high-energy factorization scheme we consider the quasi-multi-Regge kinematics (QMRK) approach [Lipatov, Kuraev, Fadin].

QMRK is based on effective quantum field theory implemented with the non-abelian gauge-invariant action, as was suggested a few years ago [Lipatov, 1995].

In the QMRK approach, $q^2 = q_T^2 = -|\mathbf{q}_T|^2 \neq 0$.

The unintegrated gluon distribution function $\Phi(x, |\mathbf{q}_T|^2, \mu^2)$ is used.

In the stage of the numerical calculations, we have used the unintegrated gluon distribution functions $\Phi(x, |\mathbf{q}_T|^2, \mu^2)$ JB , JS , and KMR.

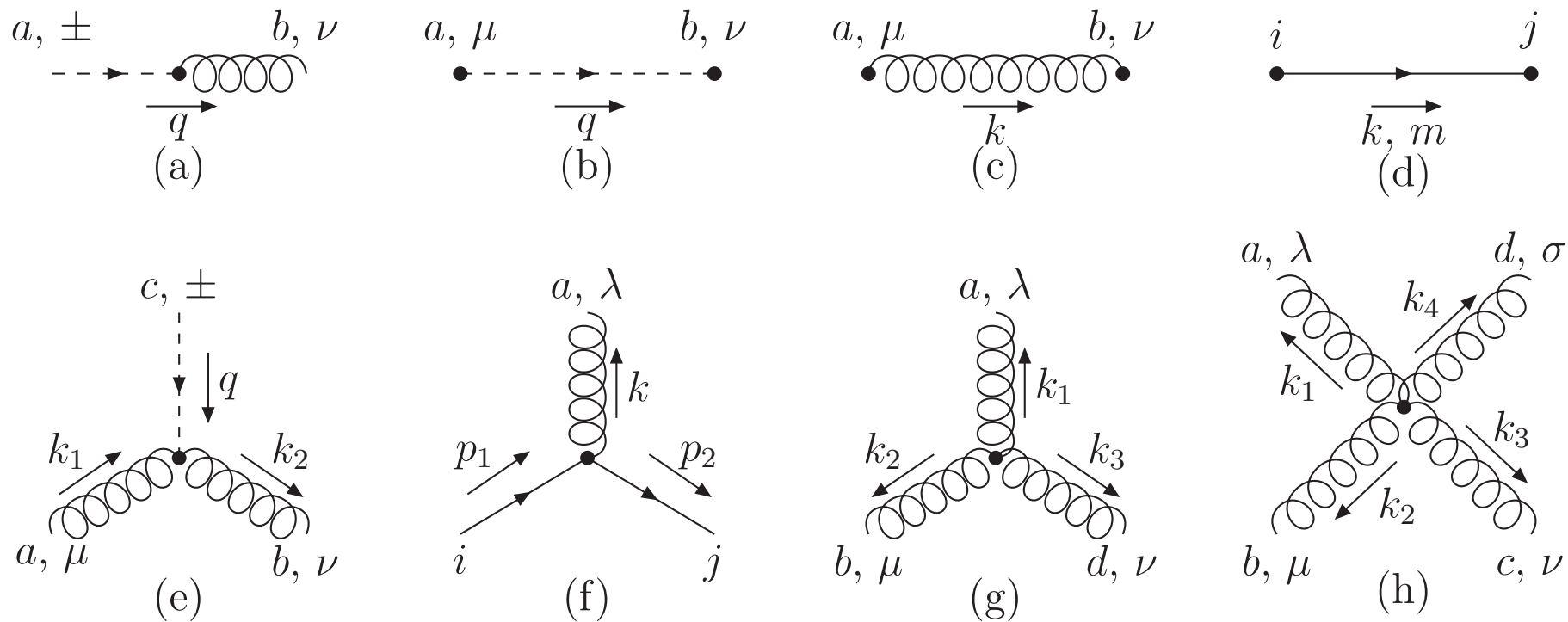
V. A. Saleev and D. V. Vasin:

- 1) Phys. Rev. D **68**, 114013 (2003);
- 2) Phys. Atom. Nucl. **68**, 94 (2005) [Yad. Fiz. **68**, 95 (2005)];
- 3) In Proc. of First Int. Workshop "HSQCD 2004", 73 (2004);
- 4) Phys. Lett. B **605**, 311 (2005);

B. A. Kniehl, V. A. Saleev and D. V. Vasin:

- 5) Phys. Rev. D **73**, 074022 (2006).
- 6) Phys. Rev. D **73**, (2006), to be published.

In 2005 the Feynman rules for the effective theory based on the non-abelian gauge-invariant action were derived for the induced and the some important effective vertices [Antonov, Kuraev, Lipatov, Cherednikov].



Feynman rules.

The induced vertices of reggeized gluon transition to Yang-Mills gluon $R^\pm \rightarrow g$ (PR-vertices) has the form:

$$\Gamma_{ab}^{\pm\nu}(q) = i\delta^{ab}q^2(n^\pm)^\nu, \quad (1)$$

$$(n^+)^\nu = P_1^\nu/E_1, \quad P_1 = E_1(1, 0, 0, 1)$$

$$(n^-)^\nu = P_2^\nu/E_2, \quad P_2 = E_2(1, 0, 0, -1)$$

$$(n^+n^-) = 2, \quad (n^\pm n^\pm) = 0,$$

$$k^\mu: k^\pm = (kn^\pm).$$

$$q_1 = q_{1T} + \frac{q_1^-}{2}n^+ = q_{1T} + x_1P_1,$$

$$q_2 = q_{2T} + \frac{q_2^+}{2}n^- = q_{2T} + x_2P_2,$$

$$q_1^+ = q_2^- = 0.$$

The induced interaction vertices of reggeized gluon with two Yang-Mills gluons (PPR-vertices) reads:

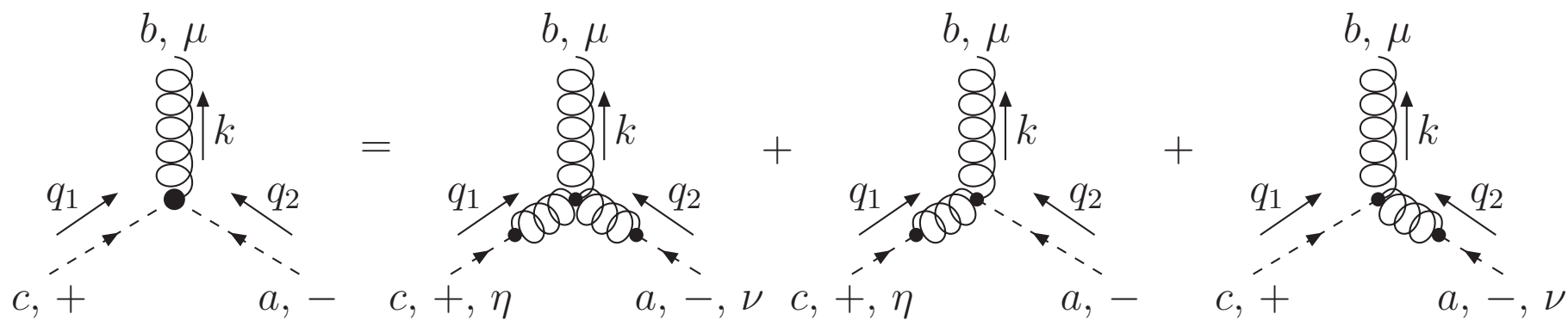
$$\Gamma_{acb}^{\mu\pm\nu}(k_1, q, k_2) = -g_s f^{abc} \frac{q^2}{k_1^\pm} (n^\pm)^\mu (n^\pm)^\nu. \quad (2)$$

The reggeized gluon propagator is specified as follows:

$$D_{ab}^{\mu\nu}(q) = -i\delta^{ab} \frac{1}{2q^2} [(n^+)^\mu (n^-)^\nu + (n^+)^\nu (n^-)^\mu], \quad (3)$$

The effective 3-vertices, which describes the production of a single gluon with momentum $k = q_1 + q_2$ and color index b in the "two reggeons collision" $R^+ R^- \rightarrow g$ (PRR-vertices):

$$\begin{aligned} \Gamma_{cba}^{+\mu-}(q_1, k, q_2) &= \\ &= V_{cab}^{\eta\nu\mu}(-q_1, -q_2, k)(n^+)^\eta(n^-)^\nu + \Gamma_{cab}^{\eta-\mu}(q_1, q_2, k)(n^+)^\eta + \Gamma_{acb}^{\nu+\mu}(q_2, q_1, k)(n^-)^\nu = \\ &= 2g_s f^{cba} \left[(n^-)^\mu \left(q_2^+ + \frac{q_2^2}{q_1^-} \right) - (n^+)^\mu \left(q_1^- + \frac{q_1^2}{q_2^+} \right) + (q_1 - q_2)^\mu \right]. \end{aligned}$$



Effective vertex $R^+ R^- \rightarrow g$.

The gauge invariance of the effective theory leads to the following condition for amplitudes in the QMRK:

$$\lim_{|\mathbf{q}_{1T}|, |\mathbf{q}_{2T}| \rightarrow 0} \overline{|\mathcal{A}(R + R \rightarrow \mathcal{H} + X)|^2} = 0. \quad (4)$$

In the QMRK approach, the hadronic cross section of quarkonium (\mathcal{H}) production in the process

$$p + p \rightarrow \mathcal{H} + X \quad (5)$$

and the partonic cross section for the reggeized-gluon fusion subprocess

$$R + R \rightarrow \mathcal{H} + X \quad (6)$$

are connected as

$$d\sigma(p + p \rightarrow \mathcal{H} + X) = \int \frac{dx_1}{x_1} \int \frac{d^2\mathbf{q}_{1T}}{\pi} \Phi(x_1, |\mathbf{q}_{1T}|^2, \mu^2) \times \\ \int \frac{dx_2}{x_2} \int \frac{d^2\mathbf{q}_{2T}}{\pi} \Phi(x_2, |\mathbf{q}_{2T}|^2, \mu^2) \times d\hat{\sigma}(R + R \rightarrow \mathcal{H} + X), \quad (7)$$

$$x_1 = \frac{q_1^-}{2E_1}, \quad x_2 = \frac{q_2^+}{2E_2}.$$

$$xG(x, \mu^2) = \int \frac{d^2\mathbf{q}_T}{\pi} \Phi(x, |\mathbf{q}_T|^2, \mu^2), \quad (8)$$

The partonic cross section for the two reggeized gluon collision can be presented as follows:

$$d\hat{\sigma}(R + R \rightarrow \mathcal{H} + X) = \frac{\mathcal{N}}{2x_1x_2S} \times \overline{|\mathcal{A}(R + R \rightarrow \mathcal{H} + X)|^2} d\Phi, \quad (9)$$

$$\mathcal{N} = \frac{(x_1x_2S)^2}{16|\mathbf{q}_{1T}|^2|\mathbf{q}_{2T}|^2}. \quad (10)$$

So that when $\mathbf{q}_{1T} = \mathbf{q}_{2T} = 0$ we obtain the conventional factorization formula of the collinear parton model:

$$d\sigma(p + p \rightarrow \mathcal{H} + X) = \int dx_1 G(x_1, \mu^2) \int dx_2 G(x_2, \mu^2) \times d\hat{\sigma}(g + g \rightarrow \mathcal{H} + X) \quad (11)$$

NRQCD formalism

The factorization hypothesis of nonrelativistic QCD (NRQCD) assumes the separation of the effects of long and short distances in heavy-quarkonium production.

NRQCD is organized as a perturbative expansion in two small parameters, the strong-coupling constant α_s and the relative velocity v of the heavy quarks.

In the framework of the NRQCD factorization approach, the cross section of heavy-quarkonium production in a partonic subprocess $a + b \rightarrow \mathcal{H} + X$ may be presented as a sum of terms in which the effects of long and short distances are factorized as

$$d\hat{\sigma}(a + b \rightarrow \mathcal{H} + X) = \sum_n d\hat{\sigma}(a + b \rightarrow Q\bar{Q}[n] + X) \langle \mathcal{O}^{\mathcal{H}}[n] \rangle, \quad (12)$$

The cross section $d\hat{\sigma}(a + b \rightarrow Q\bar{Q}[n] + X)$ can be calculated in perturbative QCD as an expansion in α_s using the non-relativistic approximation for the relative motion of the heavy quarks in the $Q\bar{Q}$ pair.

The non-perturbative transition of the $Q\bar{Q}$ pair into the physical quarkonium state \mathcal{H} is described by the NMEs $\langle \mathcal{O}^{\mathcal{H}}[n] \rangle$, which can be extracted from experimental data.

To leading order in v , we need to include the $Q\bar{Q}$ Fock states $n = {}^3S_1^{(1)}, {}^3S_1^{(8)}, {}^1S_0^{(8)}, {}^3P_J^{(8)}$ if $\mathcal{H} = \Upsilon(nS), \psi(nS)$, and $n = {}^3P_J^{(1)}, {}^3S_1^{(8)}$ if $\mathcal{H} = \chi_{bJ,cJ}(nP)$, where $J = 0, 1$ or 2 . Their NMEs satisfy the multiplicity relations

$$\begin{aligned}\langle \mathcal{O}^{\Upsilon(nS)}[{}^3P_J^{(8)}] \rangle &= (2J+1) \langle \mathcal{O}^{\Upsilon(nS)}[{}^3P_0^{(8)}] \rangle, \\ \langle \mathcal{O}^{\chi_{bJ}(nP)}[{}^3P_J^{(1)}] \rangle &= (2J+1) \langle \mathcal{O}^{\chi_{b0}(nP)}[{}^3P_0^{(1)}] \rangle, \\ \langle \mathcal{O}^{\chi_{bJ}(nP)}[{}^3S_1^{(8)}] \rangle &= (2J+1) \langle \mathcal{O}^{\chi_{b0}(nP)}[{}^3S_1^{(8)}] \rangle,\end{aligned}$$

which follow to LO in v from heavy-quark spin symmetry.

$$\langle \mathcal{O}^{\Upsilon(nS)}[{}^3S_1^{(1)}] \rangle = 2N_c(2J+1)|\Psi_n(0)|^2, \quad (13)$$

where $N_c = 3$ and $J = 1$.

$$\langle \mathcal{O}^{\chi_{bJ}(nP)}[{}^3P_J^{(1)}] \rangle = 2N_c(2J+1)|\Psi'(0)|^2. \quad (14)$$

$$d\hat{\sigma}(a + b \rightarrow Q\bar{Q}[{}^{2S+1}L_J^{(1,8)}] \rightarrow \mathcal{H}) =$$

$$d\hat{\sigma}(a + b \rightarrow Q\bar{Q}[{}^{2S+1}L_J^{(1,8)}]) \frac{\langle \mathcal{O}^{\mathcal{H}}[{}^{2S+1}L_J^{(1,8)}] \rangle}{N_{\text{col}} N_{\text{pol}}}$$

where $N_{\text{col}} = 2N_c$ for the color-singlet state, $N_{\text{col}} = N_c^2 - 1$ for the color-octet state, and $N_{\text{pol}} = 2J + 1$.

The production amplitude

$$\mathcal{A}(a + b \rightarrow Q\bar{Q}[{}^{2S+1}L_J^{(1,8)}])$$

can be obtained from the one for an unspecified $Q\bar{Q}$ state, $\mathcal{A}(a + b \rightarrow Q\bar{Q})$, by the application of appropriate projectors.

The projectors on the spin-0 and spin-1 states read:

$$\begin{aligned}\Pi_0 &= \frac{1}{\sqrt{8m^3}} \left(\frac{\hat{p}}{2} - \hat{q} - m \right) \gamma_5 \left(\frac{\hat{p}}{2} + \hat{q} + m \right), \\ \Pi_1^\alpha &= \frac{1}{\sqrt{8m^3}} \left(\frac{\hat{p}}{2} - \hat{q} - m \right) \gamma^\alpha \left(\frac{\hat{p}}{2} + \hat{q} + m \right)\end{aligned}$$

The projection operators on the color-singlet and color-octet states read:

$$C_1 = \frac{\delta_{ij}}{\sqrt{N_c}} \text{ and } C_8 = \sqrt{2}T_{ij}^c. \quad (15)$$

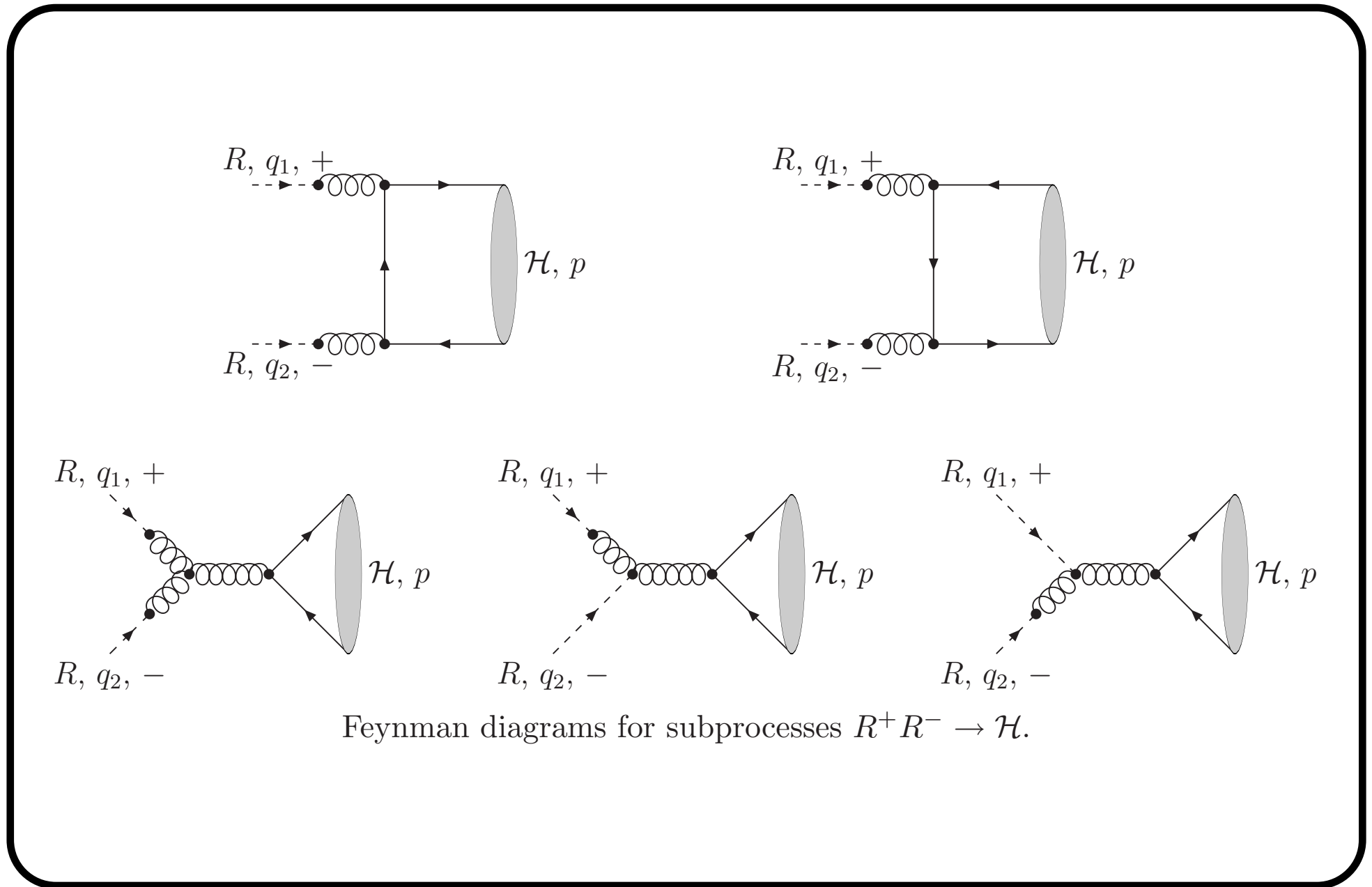
To obtain the projection on the state with orbital-angular-momentum quantum number L , we need take L times the derivative with respect to q and then put $q = 0$.

$$\begin{aligned}
& \mathcal{A}(a + b \rightarrow Q\bar{Q}[{}^1S_0^{(1,8)}]) = \\
& = \text{Tr} [C_{1,8}\Pi_0 \mathcal{A}(a + b \rightarrow Q\bar{Q})] |_{q=0}, \\
& \mathcal{A}(a + b \rightarrow Q\bar{Q}[{}^3S_1^{(1,8)}]) = \\
& = \text{Tr} [C_{1,8}\Pi_1^\alpha \mathcal{A}(a + b \rightarrow Q\bar{Q})\varepsilon_\alpha(p)] |_{q=0}, \\
& \mathcal{A}(a + b \rightarrow Q\bar{Q}[{}^3P_J^{(1,8)}]) = \\
& = \frac{d}{dq_\beta} \text{Tr} [C_{1,8}\Pi_1^\alpha \mathcal{A}(a + b \rightarrow Q\bar{Q})\varepsilon_{\alpha\beta}(p)] |_{q=0}
\end{aligned}$$

Heavy quarkonium production by reggeized gluons

In this section, we obtain the squared amplitudes for inclusive quarkonium production via the fusion of two reggeized gluons in the framework of the NRQCD. We work at LO in α_s and v and consider the following partonic subprocesses:

$$R + R \rightarrow \mathcal{H}[{}^3P_J^{(1)}, {}^3S_1^{(8)}, {}^1S_0^{(8)}, {}^3P_J^{(8)}],$$
$$R + R \rightarrow \mathcal{H}[{}^3S_1^{(1)}] + g,$$



We have obtained

$$\begin{aligned}
\overline{|\mathcal{A}(R + R \rightarrow \mathcal{H}[{}^3P_0^{(1)}])|^2} &= \frac{8}{3}\pi^2\alpha_s^2 \frac{\langle \mathcal{O}^{\mathcal{H}}[{}^3P_0^{(1)}] \rangle}{M^5} F[{}^3P_0](t_1, t_2, \varphi), \\
\overline{|\mathcal{A}(R + R \rightarrow \mathcal{H}[{}^3P_1^{(1)}])|^2} &= \frac{16}{3}\pi^2\alpha_s^2 \frac{\langle \mathcal{O}^{\mathcal{H}}[{}^3P_1^{(1)}] \rangle}{M^5} F[{}^3P_1](t_1, t_2, \varphi), \\
\overline{|\mathcal{A}(R + R \rightarrow \mathcal{H}[{}^3P_2^{(1)}])|^2} &= \frac{32}{45}\pi^2\alpha_s^2 \frac{\langle \mathcal{O}^{\mathcal{H}}[{}^3P_2^{(1)}] \rangle}{M^5} F[{}^3P_2](t_1, t_2, \varphi), \\
\overline{|\mathcal{A}(R + R \rightarrow \mathcal{H}[{}^3S_1^{(8)}])|^2} &= \frac{1}{2}\pi^2\alpha_s^2 \frac{\langle \mathcal{O}^{\mathcal{H}}[{}^3S_1^{(8)}] \rangle}{M^3} F[{}^3S_1](t_1, t_2, \varphi), \\
\overline{|\mathcal{A}(R + R \rightarrow \mathcal{H}[{}^1S_0^{(8)}])|^2} &= \frac{5}{12}\pi^2\alpha_s^2 \frac{\langle \mathcal{O}^{\mathcal{H}}[{}^1S_0^{(8)}] \rangle}{M^3} F[{}^1S_0](t_1, t_2, \varphi), \\
\overline{|\mathcal{A}(R + R \rightarrow \mathcal{H}[{}^3P_0^{(8)}])|^2} &= 5\pi^2\alpha_s^2 \frac{\langle \mathcal{O}^{\mathcal{H}}[{}^3P_0^{(8)}] \rangle}{M^5} F[{}^3P_0](t_1, t_2, \varphi), \\
\overline{|\mathcal{A}(R + R \rightarrow \mathcal{H}[{}^3P_1^{(8)}])|^2} &= 10\pi^2\alpha_s^2 \frac{\langle \mathcal{O}^{\mathcal{H}}[{}^3P_1^{(8)}] \rangle}{M^5} F[{}^3P_1](t_1, t_2, \varphi), \\
\overline{|\mathcal{A}(R + R \rightarrow \mathcal{H}[{}^3P_2^{(8)}])|^2} &= \frac{4}{3}\pi^2\alpha_s^2 \frac{\langle \mathcal{O}^{\mathcal{H}}[{}^3P_2^{(8)}] \rangle}{M^5} F[{}^3P_2](t_1, t_2, \varphi)
\end{aligned}$$

$$F^{[{}^3S_1]}(t_1, t_2, \varphi) = \frac{16t_1t_2}{(M^2 + t_1 + t_2)^2(M^2 + |\mathbf{p}_T|^2)} [(t_1 + t_2)^2 + M^2(t_1 + t_2 - 2\sqrt{t_1t_2} \cos \varphi)],$$

$$F^{[{}^1S_0]}(t_1, t_2, \varphi) = \frac{32M^2t_1t_2 \sin^2 \varphi}{(M^2 + t_1 + t_2)^2},$$

$$F^{[{}^3P_0]}(t_1, t_2, \varphi) = \frac{32M^2t_1t_2}{9(M^2 + t_1 + t_2)^4} [(3M^2 + t_1 + t_2) \cos \varphi + 2\sqrt{t_1t_2}]^2,$$

$$F^{[{}^3P_1]}(t_1, t_2, \varphi) = \frac{32M^2t_1t_2}{9(M^2 + t_1 + t_2)^4} [(t_1 + t_2)^2 \sin^2 \varphi + M^2(t_1 + t_2 - 2\sqrt{t_1t_2} \cos \varphi)],$$

$$F^{[{}^3P_2]}(t_1, t_2, \varphi) = \frac{16M^2t_1t_2}{3(M^2 + t_1 + t_2)^4} [3M^4 + 3(t_1 + t_2)M^2 + (t_1 + t_2)^2 \cos^2 \varphi + 4t_1t_2 + 2\sqrt{t_1t_2} [3M^2 + 2(t_1 + t_2)] \cos \varphi],$$

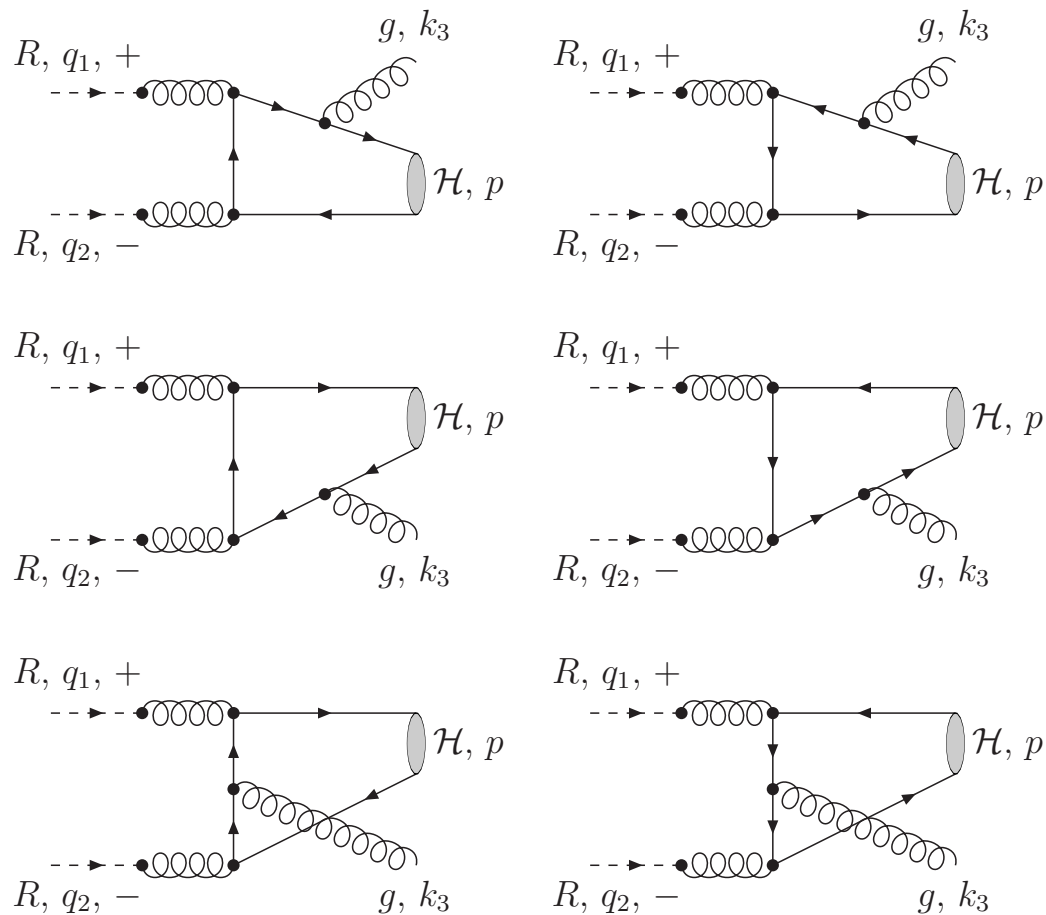
Here $\mathbf{p}_T = \mathbf{q}_{1T} + \mathbf{q}_{2T}$, $t_{1,2} = |\mathbf{q}_{1,2T}|^2$, and $\varphi = \varphi_1 - \varphi_2$ is the angle enclosed between \mathbf{q}_{1T} and \mathbf{q}_{2T} , so that

$$|\mathbf{p}_T|^2 = t_1 + t_2 + 2\sqrt{t_1 t_2} \cos \varphi$$

$$\overline{|\mathcal{A}(g + g \rightarrow \mathcal{H}[{}^{2S+1}L_J^{(1,8)}])|^2} = \lim_{t_1, t_2 \rightarrow 0} \int_0^{2\pi} \frac{d\varphi_1}{2\pi} \int_0^{2\pi} \frac{d\varphi_2}{2\pi} \mathcal{N} \times \overline{|\mathcal{A}(R + R \rightarrow \mathcal{H}[{}^{2S+1}L_J^{(1,8)}])|^2}.$$

In this way, we recover the well-known results:

$$\begin{aligned}
\overline{|\mathcal{A}(g + g \rightarrow \mathcal{H}[{}^3P_0^{(1)}])|^2} &= \frac{8}{3}\pi^2\alpha_s^2 \frac{\langle \mathcal{O}^{\mathcal{H}}[{}^3P_0^{(8)}] \rangle}{M^3}, \\
\overline{|\mathcal{A}(g + g \rightarrow \mathcal{H}[{}^3P_1^{(1)}])|^2} &= 0, \\
\overline{|\mathcal{A}(g + g \rightarrow \mathcal{H}[{}^3P_2^{(1)}])|^2} &= \frac{32}{45}\pi^2\alpha_s^2 \frac{\langle \mathcal{O}^{\mathcal{H}}[{}^3P_2^{(8)}] \rangle}{M^3}, \\
\overline{|\mathcal{A}(g + g \rightarrow \mathcal{H}[{}^3S_1^{(8)}])|^2} &= 0, \\
\overline{|\mathcal{A}(g + g \rightarrow \mathcal{H}[{}^1S_0^{(8)}])|^2} &= \frac{5}{12}\pi^2\alpha_s^2 \frac{\langle \mathcal{O}^{\mathcal{H}}[{}^1S_0^{(8)}] \rangle}{M}, \\
\overline{|\mathcal{A}(g + g \rightarrow \mathcal{H}[{}^3P_0^{(8)}])|^2} &= 5\pi^2\alpha_s^2 \frac{\langle \mathcal{O}^{\mathcal{H}}[{}^3P_0^{(8)}] \rangle}{M^3}, \\
\overline{|\mathcal{A}(g + g \rightarrow \mathcal{H}[{}^3P_1^{(8)}])|^2} &= 0, \\
\overline{|\mathcal{A}(g + g \rightarrow \mathcal{H}[{}^3P_2^{(8)}])|^2} &= \frac{4}{3}\pi^2\alpha_s^2 \frac{\langle \mathcal{O}^{\mathcal{H}}[{}^3P_2^{(8)}] \rangle}{M^3}.
\end{aligned}$$



Feynman diagrams for subprocesses $R^+ R^- \rightarrow \mathcal{H} [^3S_1^{(1)}] g$.

Heavy quarkonium production at the Tevatron

Nowadays Tevatron CDF data incorporate p_T -spectra for prompt $\Upsilon(1S, 2S, 3S)$ at the $\sqrt{S} = 1.8$ TeV and for prompt $\Upsilon(1S)$ in the different intervals of rapidity at the $\sqrt{S} = 1.96$ TeV; for direct J/ψ , for J/ψ from ψ' decays, for J/ψ from χ_{cJ} decays at the $\sqrt{S} = 1.8$ TeV; for prompt J/ψ at the $\sqrt{S} = 1.96$ TeV.

$$\begin{aligned} \sigma^{prompt}(J/\psi) = & \sigma^{direct}(J/\psi) + \sigma(\psi' \rightarrow J/\psi) + \\ & + \sigma(\chi_{cJ} \rightarrow J/\psi) + \sigma(\psi' \rightarrow \chi_{cJ} \rightarrow J/\psi) \end{aligned}$$

In contrast to previous analysis in the collinear parton model we perform a joint fit to the run-I and run-II CDF data for all p_T , including the region of small p_T , to obtain the color-octet NMEs for $\psi(nS)$, $\Upsilon(nS)$ and $\chi_{cJ}(1P)$, $\chi_{bJ}(nP)$ using three different unintegrated gluon distribution functions. Our calculations are based on exact analytical expressions for the relevant squared amplitudes, obtained in the QMRK approach.

The rapidity and pseudorapidity of a heavy quarkonium state with four-momentum $p_\mu = (p_0, \mathbf{p}_T, p_3)$ are given by

$$y = \frac{1}{2} \ln \frac{p_0 + p_3}{p_0 - p_3}, \quad \eta = \frac{1}{2} \ln \frac{|\mathbf{p}| + p_3}{|\mathbf{p}| - p_3},$$

respectively. We use also following variables

$$\xi_1 = \frac{p_0 + p_3}{2E_1}, \quad \xi_2 = \frac{p_0 - p_3}{2E_2}.$$

In the case of the $2 \rightarrow 1$ subprocesses, we obtain

$$\frac{d\sigma(p + p \rightarrow \mathcal{H} + X)}{d|\mathbf{p}_T|dy} = \frac{|\mathbf{p}_T|}{8} \int \frac{d^2\mathbf{q}_{1T}}{|\mathbf{q}_{1T}|^2} \int \frac{d^2\mathbf{q}_{2T}}{|\mathbf{q}_{2T}|^2} \Phi(\xi_1, |\mathbf{q}_{1T}|^2, \mu^2) \times \\ \times \Phi(\xi_2, |\mathbf{q}_{2T}|^2, \mu^2) \delta(\mathbf{q}_{1T} + \mathbf{q}_{2T} - \mathbf{p}_T) \overline{|\mathcal{A}(R + R \rightarrow \mathcal{H})|^2}.$$

For the $2 \rightarrow 2$ subprocess, we have

$$\frac{d\sigma(p + p \rightarrow \mathcal{H} + X)}{d|\mathbf{p}_T|dy} = \frac{|\mathbf{p}_T|}{128\pi^3} \int \frac{d^2\mathbf{q}_{1T}}{|\mathbf{q}_{1T}|^2} \int \frac{d^2\mathbf{q}_{2T}}{|\mathbf{q}_{2T}|^2} \int \frac{dx_2}{x_2 - \xi_2} \times \\ \times \Phi(x_1, |\mathbf{q}_{1T}|^2, \mu^2) \Phi(x_2, |\mathbf{q}_{2T}|^2, \mu^2) \overline{|\mathcal{A}(R + R \rightarrow \mathcal{H} + g)|^2},$$

where

$$x_1 = \frac{1}{(x_2 - \xi_2)S} \left((\mathbf{q}_{1T} + \mathbf{q}_{2T} - \mathbf{p}_T)^2 - M^2 - |\mathbf{p}_T|^2 + x_2 \xi_1 S \right).$$

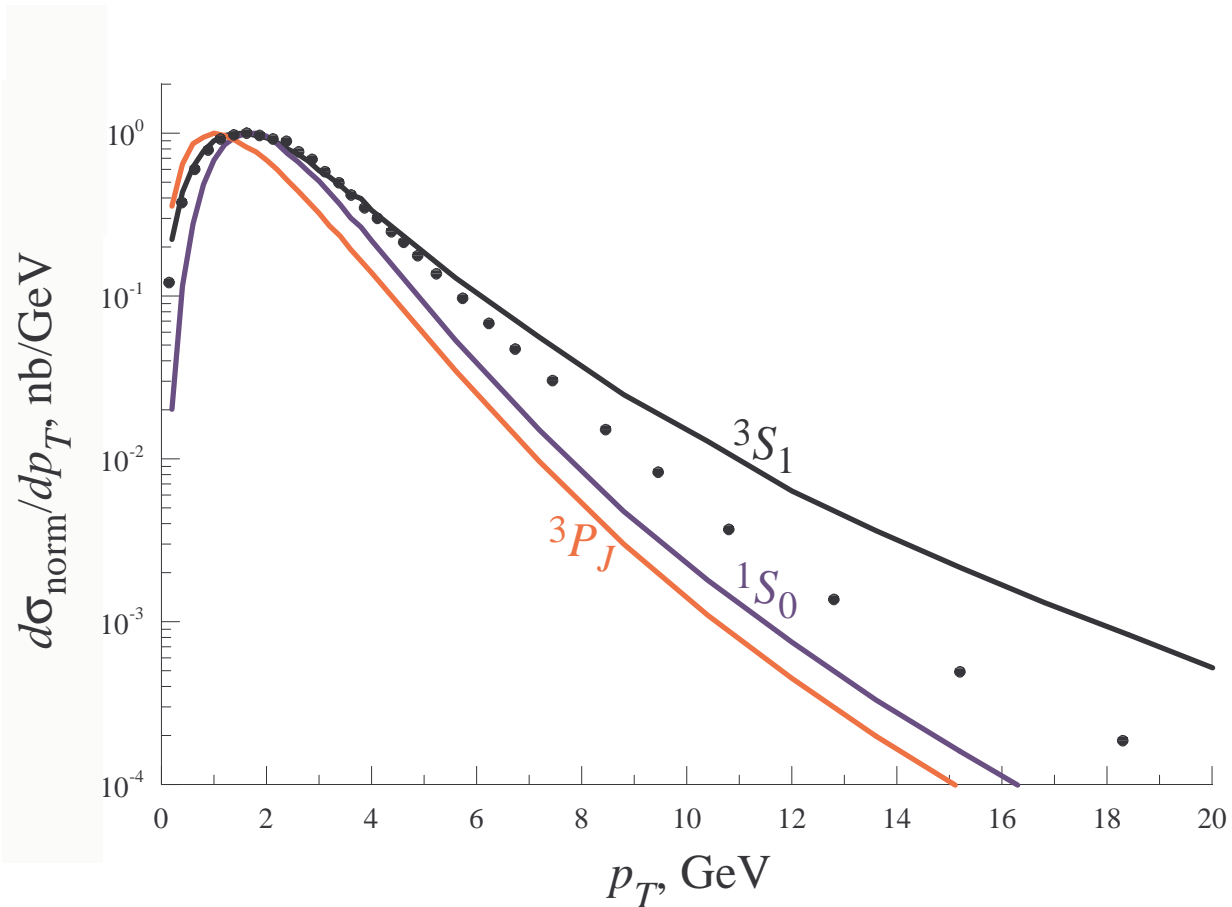
We now present and discuss our results.

In previous fits to CDF data took into consideration the region of large $|\mathbf{p}_T| > 8(4)$ GeV only, and the linear combination

$$M_r^{\mathcal{H}} = \langle \mathcal{O}^{\mathcal{H}}[{}^1S_0^{(8)}] \rangle + \frac{r}{m_Q^2} \langle \mathcal{O}^{\mathcal{H}}[{}^3P_0^{(8)}] \rangle \quad (16)$$

was fixed because it was unfeasible to separate the contributions proportional to $\langle \mathcal{O}^{\mathcal{H}}[{}^1S_0^{(8)}] \rangle$ and $\langle \mathcal{O}^{\mathcal{H}}[{}^3P_0^{(8)}] \rangle$.

By contrast, QMRK fit allow us to determine $\langle \mathcal{O}^{\mathcal{H}}[{}^1S_0^{(8)}] \rangle$ and $\langle \mathcal{O}^{\mathcal{H}}[{}^3P_0^{(8)}] \rangle$ separately, which is due to the different $|\mathbf{p}_T|$ dependence of the respective contributions for $|\mathbf{p}_T| < 8(4)$ GeV.

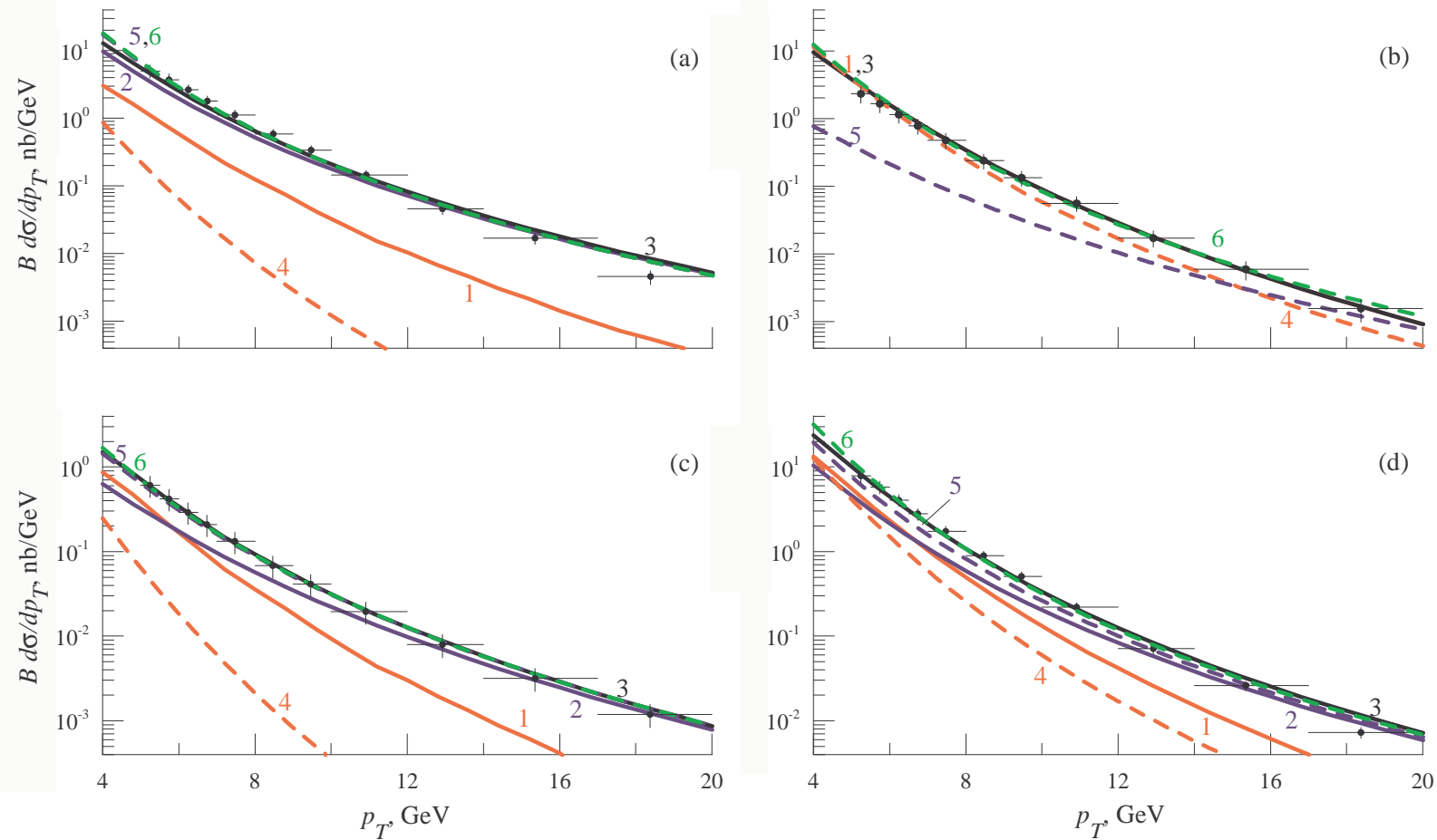


Contributions to the p_T distribution of direct $\Upsilon(1S)$ hadroproduction in $p\bar{p}$ scattering with $\sqrt{S} = 1.8$ TeV and $|y| < 0.4$ from the relevant color-octet states. All distributions are normalized on unit in their peak values.

Table: NMEs for J/ψ , ψ' and χ_{cJ}

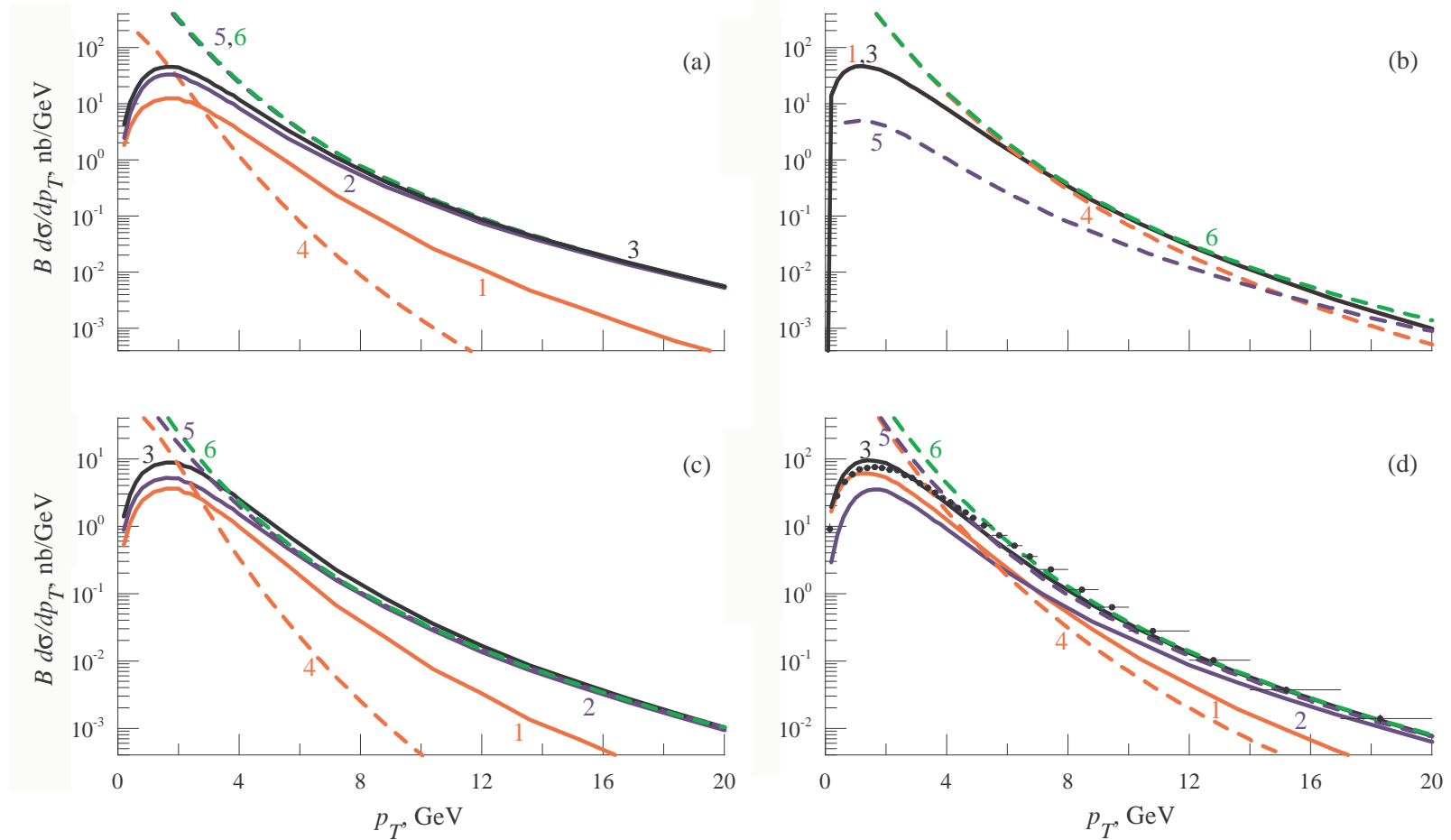
NME	PM	Fit JB	Fit JS	Fit KMR
$\langle \mathcal{O}^{J/\psi} [{}^3S_1^{(1)}] \rangle / \text{GeV}^3$	1.3	1.3	1.3	1.3
$\langle \mathcal{O}^{J/\psi} [{}^3S_1^{(8)}] \rangle / \text{GeV}^3$	$4.4 \cdot 10^{-3}$	$1.5 \cdot 10^{-3}$	$6.1 \cdot 10^{-3}$	$2.7 \cdot 10^{-3}$
$\langle \mathcal{O}^{J/\psi} [{}^1S_0^{(8)}] \rangle / \text{GeV}^3$	$4.3 \cdot 10^{-2}$	$6.6 \cdot 10^{-3}$	$9.0 \cdot 10^{-3}$	$1.4 \cdot 10^{-2}$
$\langle \mathcal{O}^{J/\psi} [{}^3P_0^{(8)}] \rangle / \text{GeV}^5$	$2.8 \cdot 10^{-2}$	0	0	0
$\langle \mathcal{O}^{\psi'} [{}^3S_1^{(1)}] \rangle / \text{GeV}^3$	$6.5 \cdot 10^{-1}$	$6.5 \cdot 10^{-1}$	$6.5 \cdot 10^{-1}$	$6.5 \cdot 10^{-1}$
$\langle \mathcal{O}^{\psi'} [{}^3S_1^{(8)}] \rangle / \text{GeV}^3$	$4.2 \cdot 10^{-3}$	$3.0 \cdot 10^{-4}$	$1.5 \cdot 10^{-3}$	$8.3 \cdot 10^{-4}$
$\langle \mathcal{O}^{\psi'} [{}^1S_0^{(8)}] \rangle / \text{GeV}^3$	$6.9 \cdot 10^{-3}$	0	0	0
$\langle \mathcal{O}^{\psi'} [{}^3P_0^{(8)}] \rangle / \text{GeV}^5$	$3.9 \cdot 10^{-3}$	0	0	0
$\langle \mathcal{O}^{\chi_{c0}} [{}^3P_0^{(1)}] \rangle / \text{GeV}^5$	$8.9 \cdot 10^{-2}$	$8.9 \cdot 10^{-2}$	$8.9 \cdot 10^{-2}$	$8.9 \cdot 10^{-2}$
$\langle \mathcal{O}^{\chi_{c0}} [{}^3S_1^{(8)}] \rangle / \text{GeV}^3$	$4.4 \cdot 10^{-3}$	0	$2.2 \cdot 10^{-4}$	$4.7 \cdot 10^{-5}$
$\chi^2/\text{d.o.f}$	–	2.2 (*)	4.1	3.0

$$\Delta L \approx \Delta S \approx 0$$



J/ψ at CDF (run I)

(a) direct, (b) χ_{cJ} -decays, (c) ψ' -decays, (d) prompt; solid lines - QMRK, dashed lines - PM; 1,4 - color-singlet, 2,5 - color-octet, 3,6 - total.



J/ψ at CDF (run II)

(a) direct, (b) χ_{cJ} -decays, (c) ψ' -decays, (d) prompt; solid lines - QMRK, dashed lines - PM; 1,4 - color-singlet, 2,5 - color-octet, 3,6 - total.

Table: Inclusive branchings fractions for transitions between spin-triplet bottomonium states.

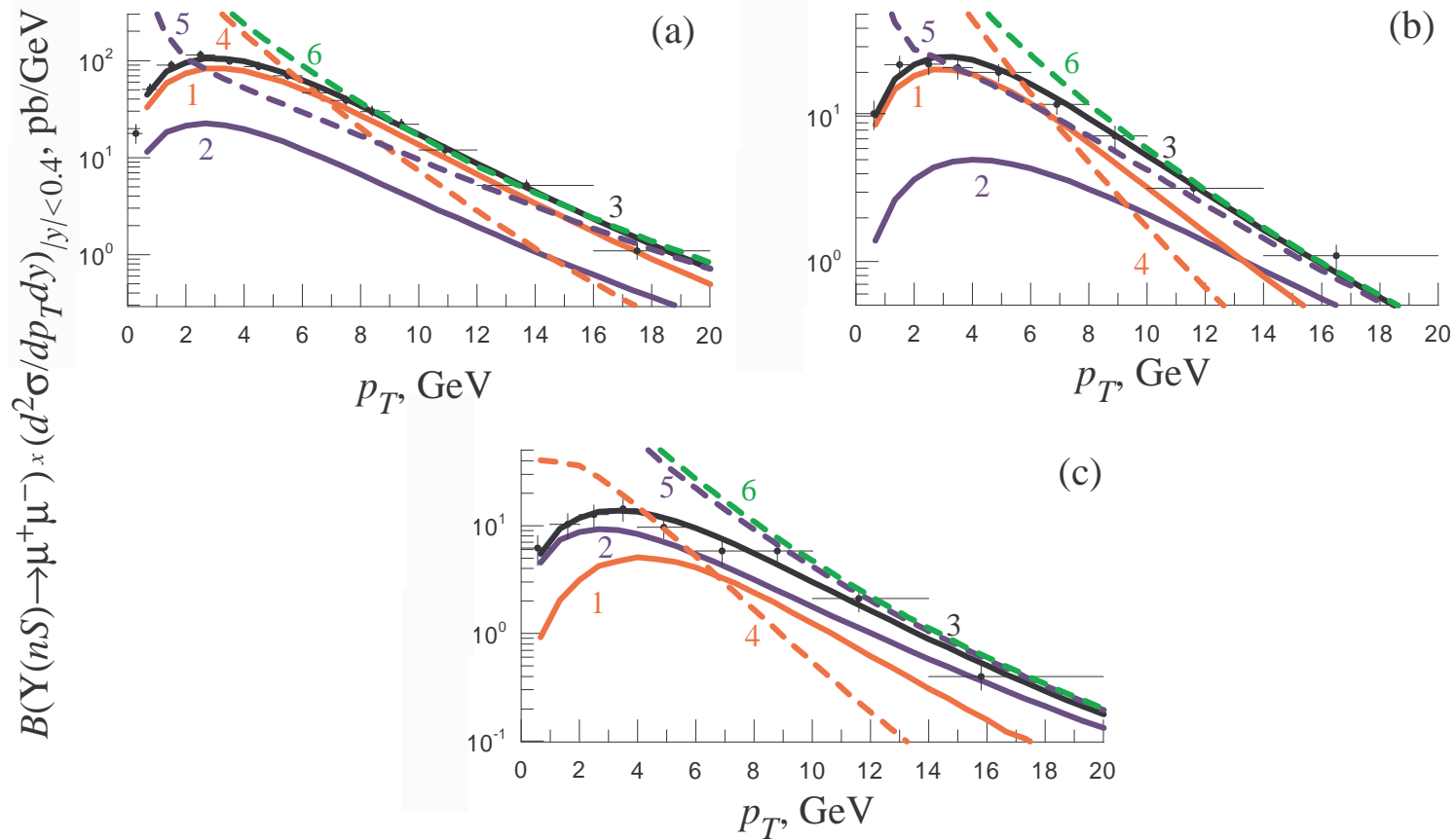
In\Out	$\Upsilon(3S)$	$\chi_{b2}(2P)$	$\chi_{b1}(2P)$	$\chi_{b0}(2P)$	$\Upsilon(2S)$	$\chi_{b2}(1P)$	$\chi_{b1}(1P)$	$\chi_{b0}(1P)$	$\Upsilon(1S)$
$\Upsilon(3S)$	1	0.114	0.113	0.054	0.106	0.007208	0.00742	0.004028	0.102171
$\chi_{b2}(2P)$	—	1	—	—	0.162	0.011016	0.01134	0.006156	0.129565
$\chi_{b1}(2P)$	—	—	1	—	0.21	0.01428	0.0147	0.00798	0.160917
$\chi_{b0}(2P)$	—	—	—	1	0.046	0.003128	0.00322	0.001748	0.0167195
$\Upsilon(2S)$	—	—	—	—	1	0.068	0.07	0.038	0.319771
$\chi_{b2}(1P)$	—	—	—	—	—	1	—	—	0.22
$\chi_{b1}(1P)$	—	—	—	—	—	—	1	—	0.35
$\chi_{b0}(1P)$	—	—	—	—	—	—	—	1	0.06
$\Upsilon(1S)$	—	—	—	—	—	—	—	—	1

Table: NMEs for $\Upsilon(1S, 2S, 3S)$, and χ_{bJ}

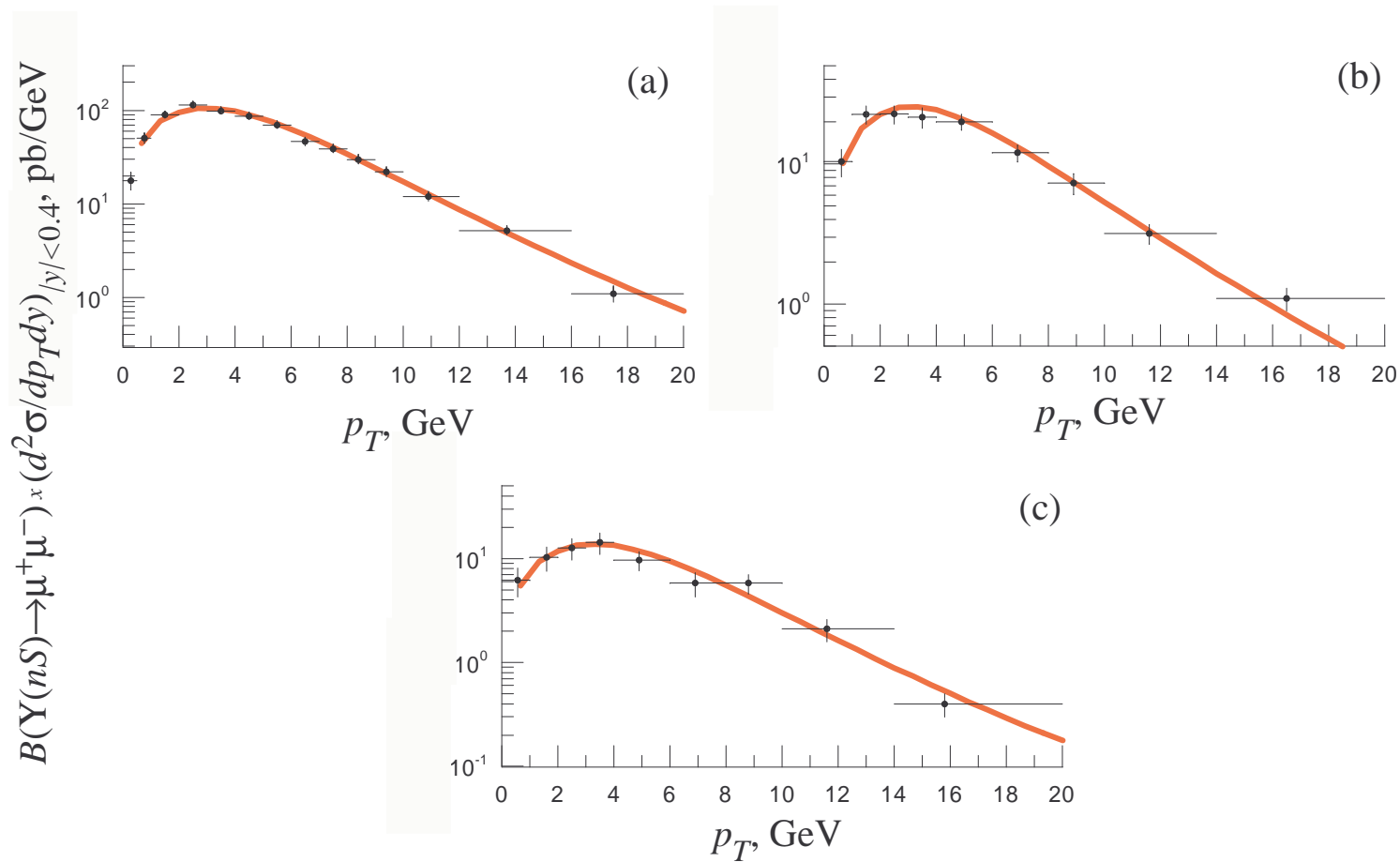
n / n	PM	Fit JB	Fit JS	Fit KMR
$\langle \mathcal{O}^{\Upsilon(1S)} [^1S_0^{(8)}] \rangle, \text{GeV}^3$	$1.4 \cdot 10^{-1}$	0.0	0.0	0.0
$\langle \mathcal{O}^{\Upsilon(1S)} [^3S_1^{(1)}] \rangle, \text{GeV}^3$	$1.1 \cdot 10^1$	$1.1 \cdot 10^1$	$1.1 \cdot 10^1$	$1.1 \cdot 10^1$
$\langle \mathcal{O}^{\Upsilon(1S)} [^3S_1^{(8)}] \rangle, \text{GeV}^3$	$2.0 \cdot 10^{-2}$	$5.3 \cdot 10^{-3}$	0.0	0.0
$\langle \mathcal{O}^{\Upsilon(1S)} [^3P_0^{(8)}] \rangle, \text{GeV}^5$	0.0	0.0	0.0	$9.5 \cdot 10^{-2}$
$\langle \mathcal{O}^{\chi_{b0}(1P)} [^3S_1^{(8)}] \rangle, \text{GeV}^3$	$1.5 \cdot 10^{-2}$	0.0	0.0	0.0
$\langle \mathcal{O}^{\chi_{b0}(1P)} [^3P_0^{(1)}] \rangle, \text{GeV}^5$	2.4	2.4	2.4	2.4
$\langle \mathcal{O}^{\Upsilon(2S)} [^1S_0^{(8)}] \rangle, \text{GeV}^3$	0.0	0.0	0.0	0.0
$\langle \mathcal{O}^{\Upsilon(2S)} [^3S_1^{(1)}] \rangle, \text{GeV}^3$	4.5	4.5	4.5	4.5
$\langle \mathcal{O}^{\Upsilon(2S)} [^3S_1^{(8)}] \rangle, \text{GeV}^3$	$1.6 \cdot 10^{-1}$	0.0	0.0	$3.3 \cdot 10^{-2}$
$\langle \mathcal{O}^{\Upsilon(2S)} [^3P_0^{(8)}] \rangle, \text{GeV}^5$	0.0	0.0	0.0	0.0
$\langle \mathcal{O}^{\chi_{b0}(2P)} [^3S_1^{(8)}] \rangle, \text{GeV}^3$	$8.0 \cdot 10^{-3}$	$1.1 \cdot 10^{-2}$	0.0	0.0
$\langle \mathcal{O}^{\chi_{b0}(2P)} [^3P_0^{(1)}] \rangle, \text{GeV}^5$	2.6	2.6	2.6	2.6
$\langle \mathcal{O}^{\Upsilon(3S)} [^1S_0^{(8)}] \rangle, \text{GeV}^3$	$5.4 \cdot 10^{-2}$	0.0	0.0	0.0
$\langle \mathcal{O}^{\Upsilon(3S)} [^3S_1^{(1)}] \rangle, \text{GeV}^3$	4.3	4.3	4.3	4.3
$\langle \mathcal{O}^{\Upsilon(3S)} [^3S_1^{(8)}] \rangle, \text{GeV}^3$	$3.6 \cdot 10^{-2}$	$1.4 \cdot 10^{-2}$	$5.9 \cdot 10^{-3}$	$1.1 \cdot 10^{-2}$
$\langle \mathcal{O}^{\Upsilon(3S)} [^3P_0^{(8)}] \rangle, \text{GeV}^5$	0.0	$2.4 \cdot 10^{-2}$	$3.4 \cdot 10^{-3}$	$5.2 \cdot 10^{-2}$
$\chi^2/\text{d.o.f}$	—	2.9	$2.7 \cdot 10^1$	$4.9 \cdot 10^{-1}$

$$\frac{\text{Color Octet Contribution}}{\text{Color Singlet Contribution}} \ll 1$$

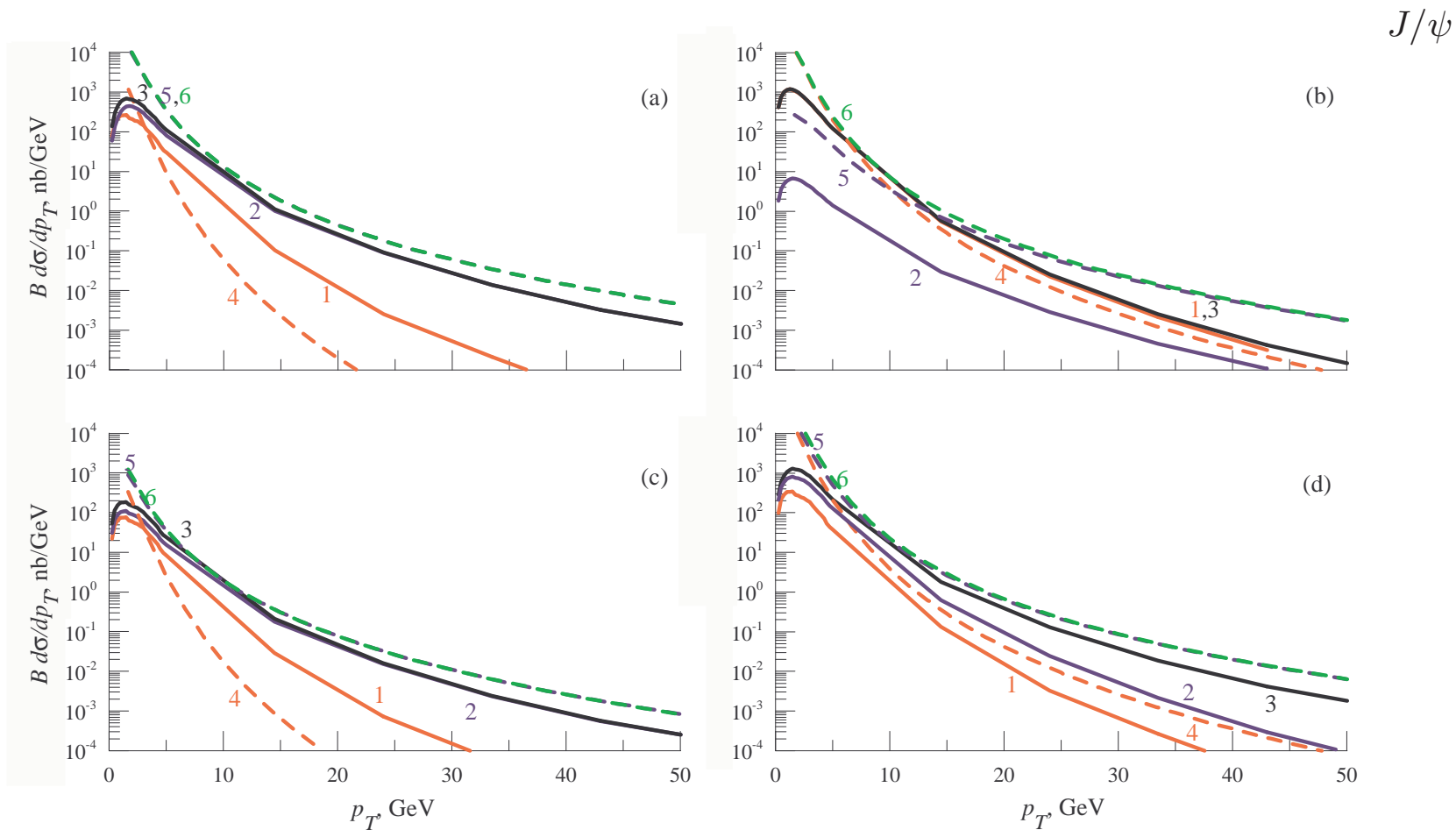
$$v_{c\bar{c}}^2 \simeq 0.3, \quad v_{b\bar{b}}^2 \simeq 0.1$$



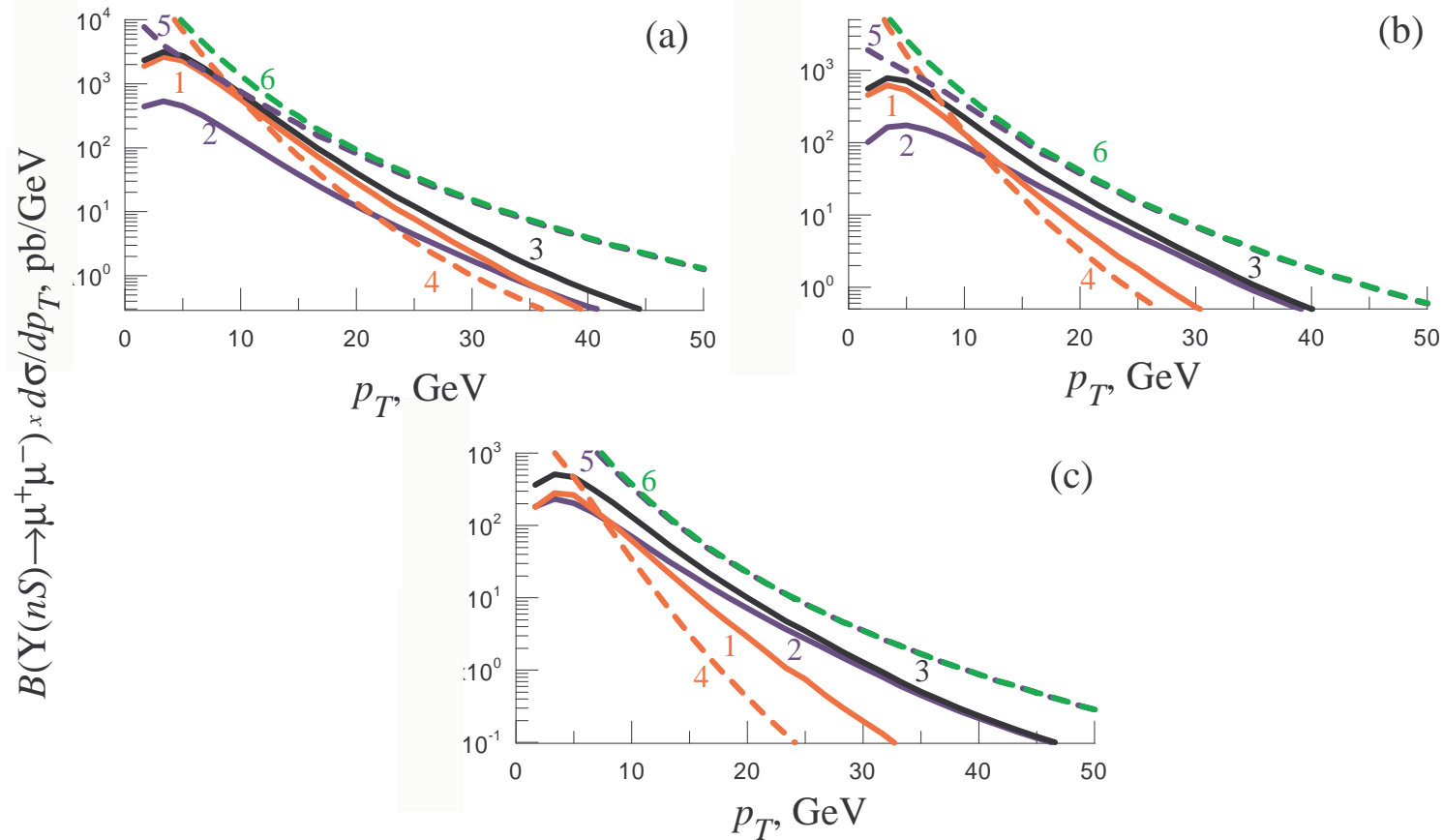
Prompt $\Upsilon(nS)$ p_T -spectra. $\Upsilon(1S)$ – a, $\Upsilon(2S)$ – b, $\Upsilon(3S)$ – c, KMR distribution function



Prompt $\Upsilon(nS)$ p_T -spectra. $\Upsilon(1S)$ – a, $\Upsilon(2S)$ – b, $\Upsilon(3S)$ – c, KMR distribution function, Color Singlet Model with $\chi_{bJ}(3P)$ contribution.



p_T -spectra at $\sqrt{S} = 14$ TeV and $|y| < 2.5$: (a) direct, (b) χ_{cJ} -decays, (c) ψ' -decays, (d) prompt; solid lines - QMRK, dashed lines - PM; 1,4 - color-singlet, 2,5 - color-octet, 3,6 - total.



Prompt Υ p_T -spectra at $\sqrt{S} = 14$ TeV and $|y| < 2.5$: (a) $\Upsilon(1S)$, (b) $\Upsilon(2S)$, (c) $\Upsilon(3S)$; solid lines - QMRK, dashed lines - PM; 1,4 - color-singlet, 2,5 - color-octet, 3,6 - total.

Conclusion

1. Working at LO in the QMRK plus NRQCD approach, we analytically evaluated the squared amplitudes of prompt heavy quarkonium production in two reggeized gluon collisions.
2. We extracted the relevant color-octet NMEs, $\langle \mathcal{O}^{\mathcal{H}}[{}^3S_1^{(8)}] \rangle$, $\langle \mathcal{O}^{\mathcal{H}}[{}^1S_0^{(8)}] \rangle$, and $\langle \mathcal{O}^{\mathcal{H}}[{}^3P_0^{(8)}] \rangle$ for $\mathcal{H} = \Upsilon(1S, 2S, 3S)$, J/ψ , ψ' , $\chi_{cJ}(1P)$ and $\chi_{bJ}(1P, 2P)$, through fits to p_T distributions measured by the CDF Collaboration in $p\bar{p}$ collisions at the Tevatron with $\sqrt{S} = 1.8$ TeV and 1.96 TeV using three different unintegrated gluon distribution functions, namely JB , JS , and KMR.
3. Our fit to the Tevatron CDF data turned out to be satisfactory with the KMR unintegrated gluon distribution function in the proton.

4. $\Delta S \simeq \Delta L \simeq 0$.

5. $\langle \mathcal{O}^{(b\bar{b})} [{}^{2S+1}L_J^{(8)}] \rangle \ll \langle \mathcal{O}^{(c\bar{c})} [{}^{2S+1}L_J^{(8)}] \rangle$

6. We have obtained heavy quarkonium production spectra at the LHC Collider in the framework of QMRK approach.

7. We have demonstrated the nontrivial phenomenological application of the QMRK approach.